Journal of Electroceramics (2023) 50:37–43
https://doi.org/10.1007/s10832-023-00302-4

Phase transition and electrical properties of high performance, high temperature $Bi(Mg,Ti)O_3$-$PbTiO_3$-$PbZrO_3$ relaxor ferroelectric ceramics

Jiao Jin[1] · Jiansheng Zhang[1] · Min Shi[1] · Chongyou Feng[1] · Yichen Huang[1]

Received: 9 November 2022 / Accepted: 29 December 2022 / Published online: 17 January 2023

Abstract
Traditional $Pb(Mg_{1/3}Nb_{2/3})O_3$-$PbTiO_3$ based relaxor ferroelectrics have attracted much attention. However, the relatively low T_m restricts their application in the high temperature range. In the present study, a novel $(0.8\text{-}x)Bi(Mg_{1/2}Ti_{1/2})O_3$-$xPbTiO_3$-$0.2PbZrO_3$ ((0.8-x)BMT-xPT-PZ) relaxor ferroelectric based on the high temperature BMT-PT piezoelectrics was designed. All samples exhibit pure perovskite structures and the phase structures show a gradual transition from relaxor rhombohedral (R) to normal tetragonal (T) phases via the morphotropic phase boundary (MPB) in the composition range x = 0.36–0.39. The dielectric relaxation behavior can be observed in all samples although a spontaneous normal-relaxor ferroelectric transformation is observed in the T phase region. The x = 0.38 sample exhibits the optimal overall electrical properties with the d_{33} value of 325 pC/N, the k_p value of 0.38, the T_m value of 290 °C. The results indicate that the present studied ternary system has a good potential as high temperature relaxor ferroelectrics.

Keywords Relaxor ferroelectric · High T_m · Morphtropic phase boundary · Electrical properties

1 Introduction

There has been increasing interest in relaxor ferroelectrics in the past few years owing to their interesting physical properties from an application point of view [1–4]. Relaxor ferroelectrics show particular features that different from normal ferroelectrics, characterized by the diffuse phase transition with broad peak of dielectric constant, as well as the significant frequency dependence of the dielectric response, which shifts towards higher temperature with increasing the measurement frequency [1, 5]. Currently, the dominating studies on relaxor ferroelectrics are focused on the solid solutions that composed of the relaxor $Pb(B_IB_{II})O_3$ and ferroelectric $PbTiO_3$ (PT), such as $Pb(Mg_{1/3}Nb_{2/3})O_3$-$PbTiO_3$ (PMN-PT), $Pb(Zn_{1/3}Nb_{2/3})O_3$-$PbTiO_3$ (PZN-PT). These materials show high dielectric constants, high electrostriction coefficients and large piezoelectric coefficients. Unfortunately, the temperature of the maximum dielectric constant (T_m) of mostly Pb-based perovskite relaxors ferroelectrics is about 140-175°C [6], which is not high enough to use these materials in high temperature fields such as automotive, aerospace, and related industrial applications that need wide working temperature range. A series of high Curie temperature relaxor ferroelectrics materials are thus developed based on the binary solid solution between relaxor $Pb(Sc_{1/2}Nb_{1/2})O_3$ (PSN), $Pb(In_{1/2}Nb_{1/2})O_3$ (PIN), and $Pb(Yb_{1/2}N_{1/2})O_3$ (PYN) and ferroelectric PT and the ternary system $Pb(In_{1/2}Nb_{1/2})O_3$-$Pb(Mg_{1/3}Nb_{2/3})O_3$-$PbTiO_3$ (PIN-PMN-PT) [6–10]. These materials possess relative high Curie temperature on the order of 260–350 °C and excellent electrical properties near the morphotropic phase boundary (MPB) composition.

The recent discovery of high temperature piezoelectric materials based on the solid solution between primary (or complex) Bi-based perovskite structure $(Bi(Me)O_3$ or $Bi(B'B'')O_3)$ and ferroelectric $PbTiO_3$ end members should provide another strategy to develop high-temperature relaxor ferroelectric materials [11, 12]. $Bi(Mg_{1/2}Ti_{1/2})O_3$-$PbTiO_3$ is a typical high Curie temperature ferroelectric system, which exhibits higher ferroelectric-paraelectric phase transition temperature up to 478 °C with composition near the MPB [13]. However, no obvious dielectric frequency dispersion behavior existed although the system shows obvious broad dielectric maximum. It is widely accepted that

✉ Jiao Jin
jin871127jiao@163.com

[1] Intelligent Manufacturing College, Jiaxing Vocational & Technical College, 314036 Jiaxing, P.R. China

the polarization in relaxor ferroelectrics is associated with the behavior of the polar regions in the materials, i.e., polar nanoregions (PNRs). Randall et al. have found that the domain structure of the rhombohedral phase BMT-PT consists of dark and white regions of polar microdomain structure with a domain size ~ 50nm, which is much higher than the size of the PNRs in the traditional Pb-based relaxors but smaller than the size of the macrodomain in the tetragonal BMT-PT [13]. In addition, these microdomains should also have a frozen-in polarization rather than dynamic state owing to the absence of the frequency dispersion of the dielectric data. Therefore, this behavior of broadening of the dielectric peak without frequency dispersion should be indicated as diffused phase transition (DFT) (an intermediate state between normal and relaxor ferroelectrics) and it is expected that the dielectric relaxation behavior can be induced by introducing the heterogeneous ions [14].

In this study, a ternary $Bi(Mg_{1/2}Ti_{1/2})O_3$-$PbTiO_3$-$PbZrO_3$ (BMT-PT-PZ) system is introduced. Comparing with other BMT-PT-based systems, PZ has the relatively high Curie temperature and the large spontaneous polarization within subcell. These characteristics would be beneficial for obtaining high-temperature relaxor ferroelectric ceramics. All compositions show relatively high Curie temperature and the obvious dielectric relaxation behavior can be observed in both rhombohedral and tetragonal phase regions. In addition, a spontaneous normal-relaxor ferroelectric transformation can be detected in some compositions near the tetragonal phase region. The phase transition behavior and the corresponding evolution of various electrical properties were systematically investigated.

2 Experimental

The ternary $(0.8\text{-}x)Bi(Mg_{1/2}Ti_{1/2})O_3$-$xPbTiO_3$-$0.2PbZrO_3$ ((0.8-x)BMT-xPT-PZ) ceramics ($x = 0.31$–0.45) were prepared by the conventional mixed-oxide techniques by using the reagent-grade metal oxides and carbonate powders of PbO, Bi_2O_3, TiO_2, ZrO_2 and $(MgCO_3)_4.Mg(OH)_2.5H_2O$ as the starting raw materials. These powders were ball milled with ZrO_2 balls for 4 h using ethanol as the medium. After drying, they were calcined at 835 °C for 4 h and then ball milled again for 6 h with the addition of PVB binder. The powders were pressed into pellets 10 mm in diameter and 0.8–1.2 mm in thickness under uniaxial pressure. All pellets were sintered in air in the temperature range of 1025–1125 °C for 2 h. For electrical measurements, silver paste was painted on major sides of the samples and fired at 550 °C for 30 min.

The phase structure of the sintered samples was identified by X-ray powder diffractometer (XRD, D/MAX2500VL/PC, Rigaku, Tokyo, Japan). The scanning rate of the full pattern (2θ range from 20° to 80°) was 4° min^{-1}. The Microstructure was observed by using a scanning electron microscope (SEM, JEOL JSM-6490LV, Tokyo, Japan). Temperature dependence of dielectric constants at various frequencies were measured by an LCR meter (E4980A) connected to a computer automatic measurement. The ferroelectric hysteresis loops and the strain versus electric field curves were measured at room temperature using a ferroelectric tester (Precision LC, Radiant Technologies Inc., Albuquerque, NM) connected with a laser interferometric vibrometer (SP-S 120, SIOS technik GmbH, Germany). The piezoelectric coefficient d_{33} and electromechanical properties k_p were measured by a Belincourt meter (YE2730A, Sinocera, Yangzhou, China) and an impedance analyzer (PV70A, Beijing Band ERA Co. Ltd., Beijing, China), respectively. The poled samples were annealed at different temperature for 5 min and the d33 values were then measured again after being cooled to room temperature.

3 Results and discussion

Figure 1 shows the SEM images of (0.8-x)BMT-xPT-0.2PZ ceramics with selected x content sintered at 1070 °C. All samples are well densified with little pores and the average grain size shows a slight increase with the addition of PT from ~ 3.5 μm at $x = 0.31$ ~ 6.6 to μm at $x = 0.45$. However, in the studied composition range, the grains are well developed and closely compacted, the grain size distribution is uniform and the grain boundary is clear in all samples.

Figure 2(a) shows the room temperature x-ray diffraction patterns of (0.8-x)BMT-xPT-0.2PZ ceramics in the two-theta range of 20-60°. All samples exhibit a pure perovskite structure without any secondary phases. However, a distinct phase structure change can be observed with changing the PT content. A pure rhombohedral (R) phase characterized by the single $(200)_R$ peak can be observed as the x content is below 0.36, whereas, a pure tetragonal (T) phase characterized by an obvious $(200)_{pc}$ doublet corresponding to the $(002)_T$ and $(200)_T$ reflections can be observed as $x > 0.39$. As a result, the morphotropic phase boundary (MPB) between the R and T phases is identified in the composition range of $0.36 \le x \le 0.39$. To estimate the phase structure evolution within MPB, enlarged XRD patterns of samples with $0.36 \le x \le 0.39$ in the 2θ range of 44-46° fitted by the Peakfit software package are shown in Fig. 2(b). Three peaks corresponding to the $(200)_T$, $(200)_R$ and $(002)_T$ from low angle side to high angle side, respectively, can be obtained, confirming the coexistence of the R and T phases in this composition range. The evolution of lattice parameters and the corresponding lattice distortion is shown in Fig. 3. It

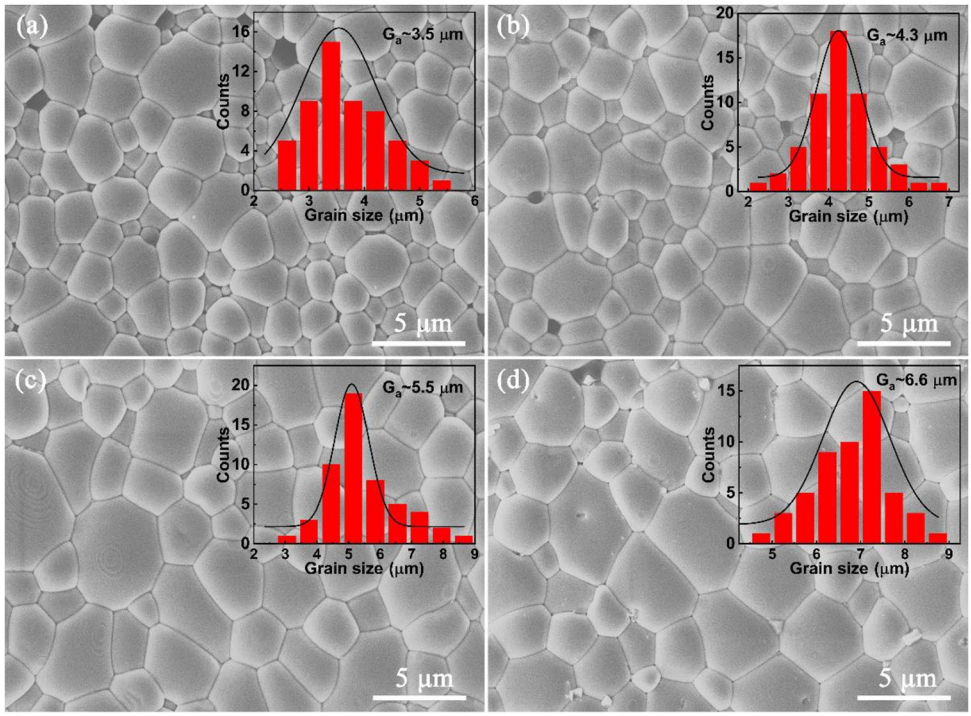

Fig. 1 SEM micrographs of natural surface in (0.8-x)BMT-xPT-0.2PZ ceramics sintered at 1075 °C: (a) x = 0.33, (b) x = 0.35, (c) x = 0.38, (d) x = 0.40

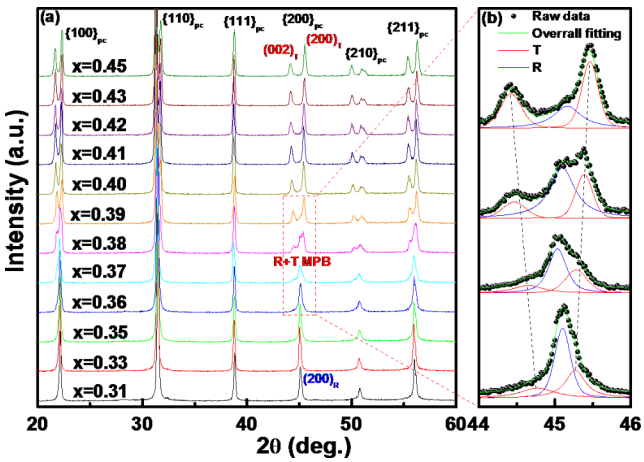

Fig. 2 (a)The room temperature XRD data of (0.8-x)BMT-xPT-0.2PZ ceramics as a function of x, and (b) the evolution of $\{200\}_{pc}$ reflections within the MPB.

can be seen that a_R axis of R phase shows little composition dependence, whereas, both a_T and c_T axes in T phase change drastically with varying x once the T phase is appeared. As $x \geq 0.36$, the increase of x induces a drastic increase of c_T axis but an obvious decrease of a_T axis, leading to the monotonous increase of tetragonality (c/a ratio). This can be confirmed by the continuously enlarged splitting between $(002)_T$ and $(200)_T$ reflections as shown in Fig. 2(a).

Figure 4 shows the temperature dependence of dielectric constant and loss tangent of (0.8-x)BMT-xPT-0.2PZ. The corresponding phase diagram is shown in Fig. 5. With increasing x, T_m value exhibits a slight increase from ~270 °C at x = 0.31 to ~360 °C at x = 0.45. Most importantly, the T_m value of MPB compositions is near 300 °C, which is much higher than that of Pb-based relaxor ferroelectric MPB compositions. In the R phase region ($x \leq 0.35$), the dielectric behavior of these specimens exhibits the prototypical relaxor characteristics with strongly diffuse phase transition and the frequency dispersion behaviors. It should be noted that these sample show a relatively high temperature of the dielectric maximum (Tm) large than 270 °C, which increases monotonously with increasing the PT content. This temperature is much higher than the T_m value in traditional Pb-based relaxor ferroelectrics. Similar to the R phase region, all samples in MPB (x = 0.36–0.39) also show broad dielectric peaks as well as an obvious frequency dispersion near T_m. However, once the R phase is disappeared ($x \geq 0.40$), an extra dielectric peak can be observed in both ε_r-T and tan δ-T curves. It can be seen from Fig. 4(d-f) that there exists a critical temperature below T_m, characterized by the sharp increase of dielectric constant similar to that of observed ferroelectric-paraelectric phase transition in normal ferroelectrics. This temperature is indicated as T_{fr}, where the subscript fr is designated to imply the spontaneous transformation from a normal ferroelectric phase to relaxor [15, 16]. As temperature is below T_{fr}, no dielectric dispersion is observed similar to that of temperature dependent dielectric behavior in normal ferroelectrics. It should be noted that pronounced dielectric dispersion near the T_m is still existed although these sample exhibits a single T phase at room temperature. Also, there exists the rapid increase

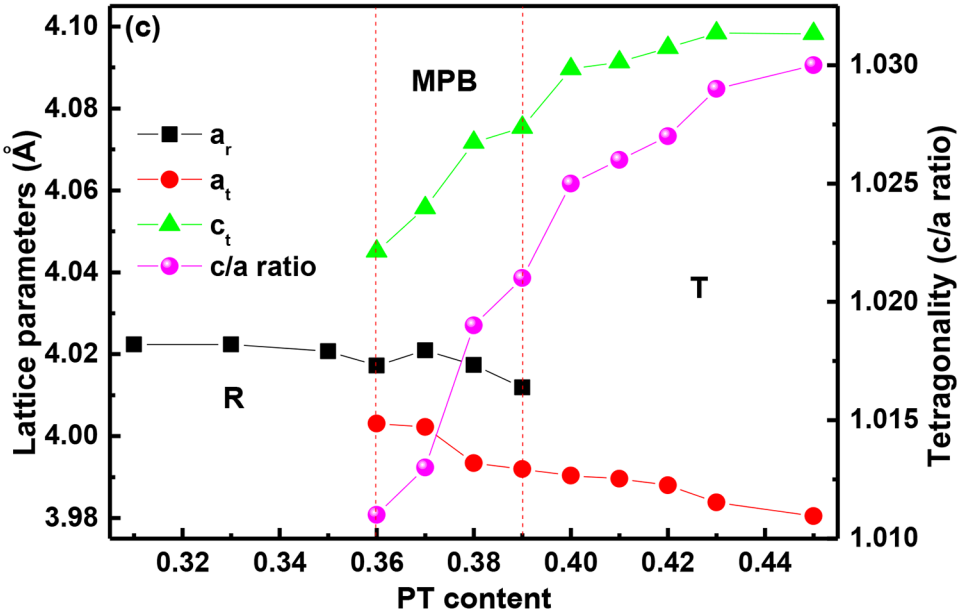

Fig. 3 The evolution of lattice parameters as a function of x

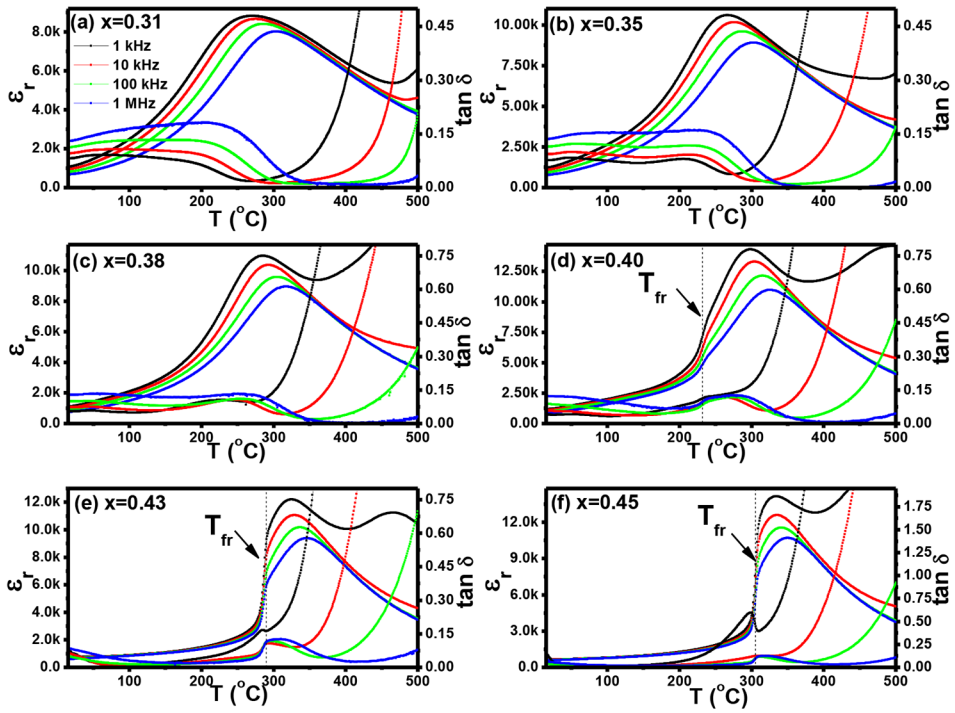

Fig. 4 Temperature dependent dielectric constant and loss tangent of selected (0.8-x)BMT-xPT-0.2PZ ceramics with different frequencies

in the temperature dependent of dielectric constant, corresponding to the T_{fr} that defined above. As can be seen, T_{fr} shows frequency independent and only changes with the variation the PT content. In addition, although both T_{fr} and T_m increase with increasing the PT content, simultaneously, they tend to merge into a single one. The extent of rapid increase in the relative dielectric constant at T_{fr} is crescent as the PT content increases. Such phenomenon is similar to that of La-modified tetragonal $Pb(Zr,Ti)O_3$ and PZ modified BMT-PT [17, 18]. Besides the simply perovskite structure, the phenomenon is also observed in some complex ternary and quaternary PZT-based systems [15, 16]. Therefore, it is believed that the mechanism of the spontaneous relaxor-normal ferroelectric transformation in the present studied compositions should be similar to that of complex ternary and quaternary PZT-based systems.

Relaxor ferroelectrics are generally characterized by the broad maximum of the temperature dependent dielectric

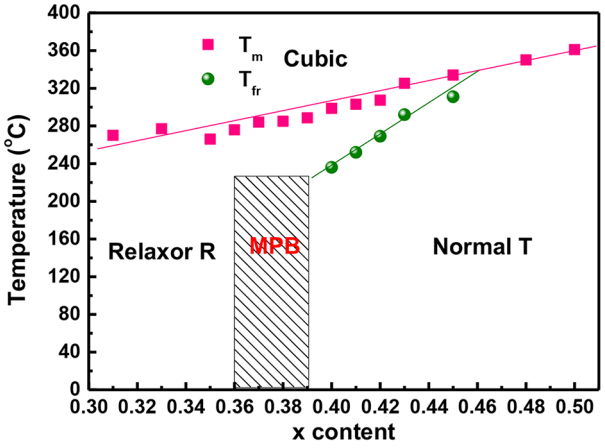

Fig. 5 The phase diagram of (0.8-x)BMT-xPT-0.2PZ ceramics

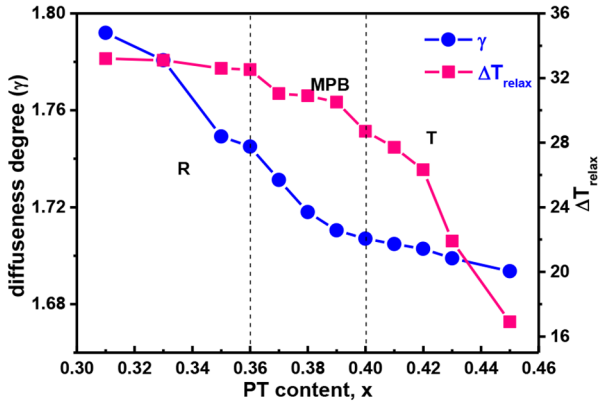

Fig. 6 The evolution of γ and ΔT_{relax} as a function of x

constant (i.e., diffuse phase transition) as well as the strong dielectric dispersion. The temperature-dependent dielectric constant of these materials deviates from the Curie-Weiss law but follows the modified Curie-Weiss law in the vicinity of T_m, which can describe the diffuseness of the phase transition [19].

$$\frac{1}{\varepsilon} - \frac{1}{\varepsilon_m} = \frac{(T - T_m)^\gamma}{C}, 1 \le \gamma \le 2 \quad (1)$$

where C is the Curie constant, and the parameter γ gives information on the degree of diffuseness, ranging from 1 for a normal Curie-Weiss law to 2 for a complete diffuse phase transition. The calculated γ is shown in Fig. 6. With increasing the PT content, γ value tends to decreases gradually. The phenomenon is similar to the observed dielectric response in PMN-PT system, where the diffuseness degree of the materials was decreased with increasing the PT content [20]. A rapid drop of the γ value is observed in the R-rich side composition, which should be attributed to the phase

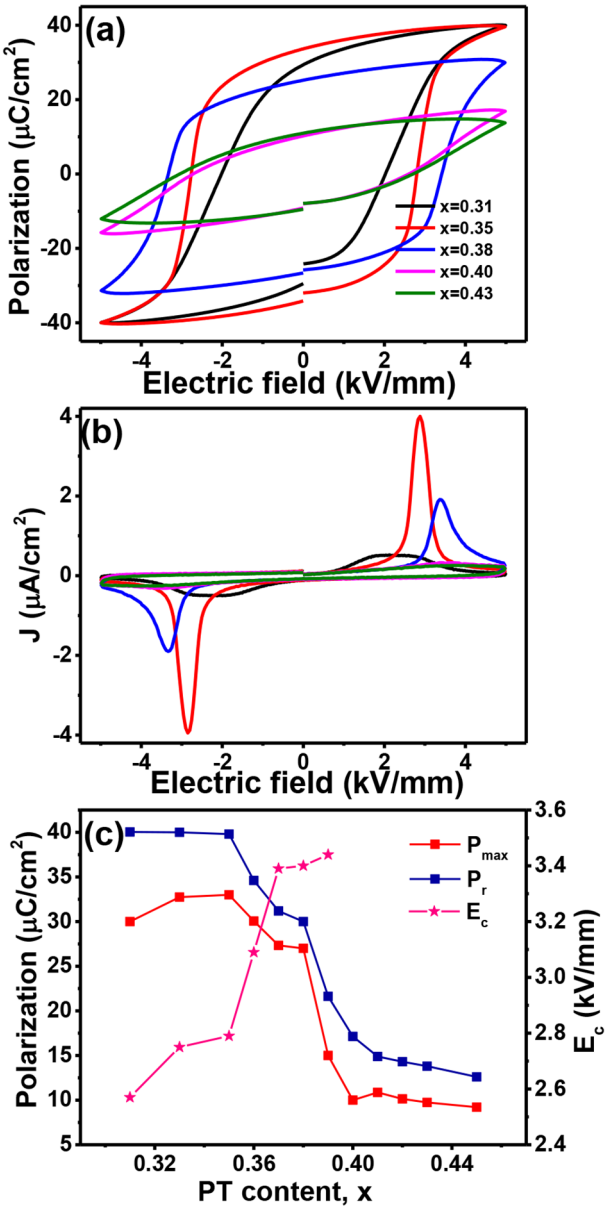

Fig. 7 (a) The bipolar P-E loops and (b) J-E curves for selected (0.8-x) BMT-xPT-0.2PZ ceramics and (c) the corresponding evolution of P_{max}, P_r, E_c as a function of x

structure change from single rhombohedral phase to MPB. By comparison, the γ value shows a relatively slow decrease in the T phase region, possibly because that T_{fr} is existed in this composition range.

The parameter ΔT_{relax} was introduced to characterize the degree of relaxor characteristics in the frequency range of 1 kHz to 1 MHz, is described as:

$$\Delta T_{relax} = T_{\varepsilon_{m(1\,MHz)}} - T_{\varepsilon_{m(1\,kHz)}} \quad (2)$$

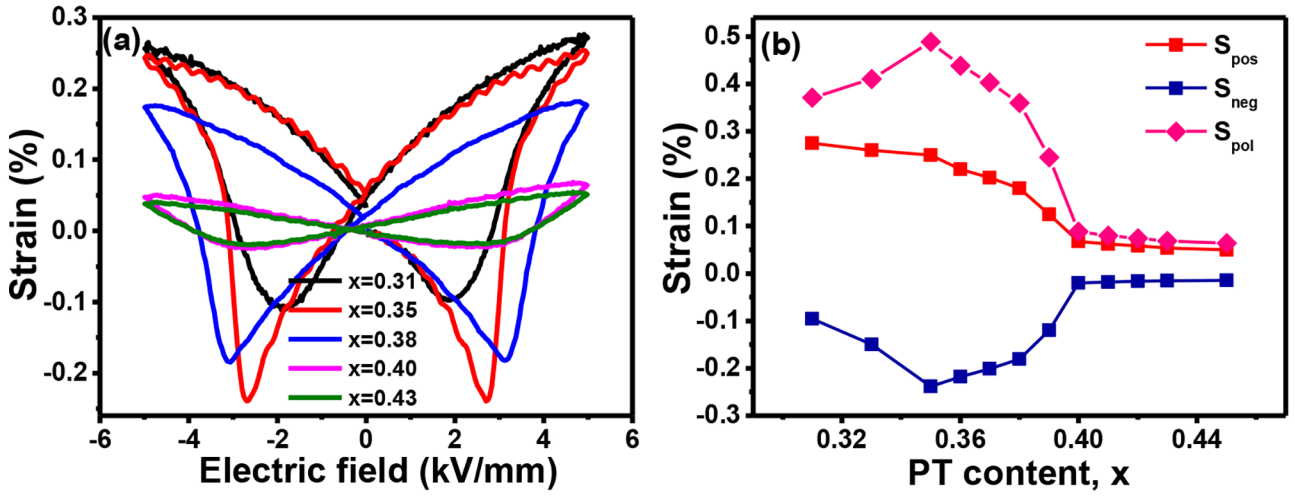

Fig. 8 (a) The bipolar S-E curves for (0.8-x)BMT-xPT-0.2PZ ceramics and (d) the corresponding evolution of S_{pos}, S_{neg}, and S_{pol} as a function of x

It can be seen from Fig. 6 that ΔT_{relax} decreases slowly in the R phase region and MPB region, indicating that the samples in these composition ranges is the typical relaxor ferroelectrics. By comparison, ΔT_{relax} decreases rapidly in the T phase region with increasing x, possibly because that relaxor R phase is absent at room temperature, but only existed in the high temperature range.

The bipolar P-E, J-E curves and the corresponding evolution of the various polarization values, and the bipolar S-E curves and the corresponding evolution of the various strain values are shown in Figs. 7 and 8, respectively. In the R phase region, the samples exhibit typical square-like P-E loops and the butterfly S-E curves with relatively large saturate polarization P_{max}, remanent polarization P_r, positive strain S_{pos}, negative strain S_{neg}, and poling strain S_{pol}. In addition, as the compositions get closer to MPB, P-E loops became more rectangular, leading the higher P_r values. This can be attributed to the easier reorientation of polarization vectors due to the flattening of free energy profile within MPB [21–23]. However, once the T phase is appeared, owing to the rapid increase of the c/a ratio of T phase with increasing x, the coercive field E_c of sample increases rapidly even in MPB region, resulting in the rapidly decrease of not only P_{max}, P_r values but also the S_{neg}, and S_{pol} values. This indicates that large c/a ratio can strongly restrict the domain switching [24]. With further increasing x, once the compositions are divorced from MPB, only unsaturated P-E loops can be observed possibly because of the high c/a ratio of the samples. The restriction of domain switching can be also confirmed by the J-E curves, in which the peak value of J-E curves decreases rapidly with increasing the c/a ratio. More importantly, no obvious peak value can be observed in J-E curves once $x \geq 0.40$, indicating that the applied electric field amplitude is not sufficient to reorient the domain

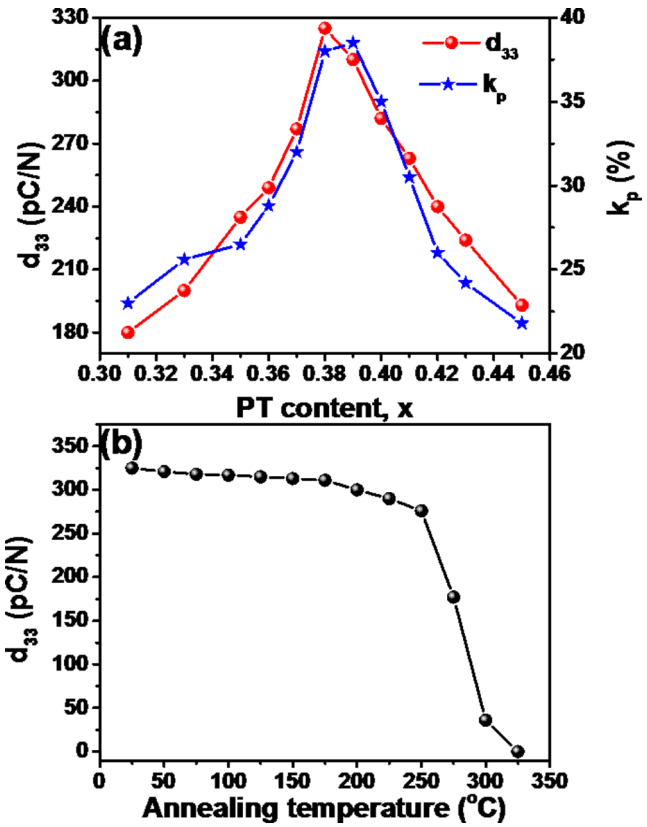

Fig. 9 (a) The evolution of d_{33} and k_p values as a function of x, and (b) the evolution of d_{33} value at different annealing temperatures

switching, i.e., no obvious domain switching occurred. It also should be noted that only two current peaks in the whole electric field cycle can be observed for all compositions, indicating that the composition modulated relaxor ferroelectric should be nonergodic relaxor state. This can be

easily understood by taking into account of their relatively high T_m.

Figure 9(a) shows the piezoelectric and electromechanical properties of poled (0.8-x)BMT-xPT-0.2PZ samples. The electrical properties display a strong compositional dependence. The best electrical property of this system was obtained at the composition within MPB with x = 0.38, which exhibits a piezoelectric constant d_{33} of 325 pC/N, a planar electromechanical coupling factor k_p of 0.38. Temperature stability of piezoelectric properties for the optimized ceramic composition is shown in Fig. 9(b). It is worth noting that d_{33} values decrease only slightly with increasing the annealing temperature until T > 200 °C, beyond which they decrease relatively fast possibly because that the sample undergoes the T_{fr}. Although the dielectric anomaly corresponding to T_{fr} in this sample is smear, it still can be speculated according to the variation trend of T_{fr}. The similar deterioration of d_{33} value can be also observed in PMN-PT based relaxor ferroelectrics because that the sample would undergo T_{R-T} [25]. However, the T_{R-T} is only 100°C, which is far below the T_{fr} in the presently studied composition. According to the aforementioned results, the present studied ternary system has a potential as high temperature relaxor ferroelectrics.

4 Conclusion

The phase transition behavior and the various electrical properties of (0.8-x)BMT-xPT-PZ ceramics were investigated in detail. The samples exhibit an obvious phase transition from R phase to T phase with increasing PT content, which is accompanied by a relaxor-normal ferroelectric transition. The R-T coexisted MPB is identified in the composition range of range x = 0.36–0.39, and the x = 0.38 sample with the protypical characteristics of relaxor ferroelectric exhibits the optimal overall electrical properties with the d_{33} value of 325 pC/N, the k_p value of 0.38, the T_m value of 290 °C. The results indicate that the present studied ternary system has a good potential as high temperature relaxor ferroelectrics.

Acknowledgements This work was supported by the "Innovation Jiaxing Talent Support Plan" High skilled Top Talent Project (No. 2241101).

Data availability The datasets in the current study are available from the corresponding author on reasonable request.

Declarations

Conflict of interest There are no conflicts of interest to declare.

References

1. C.J. Stringer, T.R. Shrout, C.A. Randall, J. Appl. Phys. **101**, 054107 (2007)
2. Z.H. Yao, H.X. Liu, Y. Liu, Z.H. Wu, M.H. Cao, H. Hao, Appl. Phys. Lett. **92**, 142905 (2008)
3. H.L. Du, W.C. Zhou, F. Luo, D.M. Zhu, S.B. Qu, Y. Li, Z.B. Pei, J. Appl. Phys. **104**, 044104 (2008)
4. J. Ryu, S. Priya, K. Uchino, Appl. Phys. Lett. **82**, 251 (2003)
5. L.E. Cross, 151, 305–320 (1994)
6. Y. Yamashita, K. Harada, Jpn J. Appl. Phys. **36**, 6039–6042 (1997)
7. N. Yasuda, H. Ohwa, D. Hasegawa, H. Hosono, Y. Yamashita, M. Iwata, Y. Ishibashi, Ferroelectrics **270**, 247–252 (2002)
8. Y. Yamamoto, S. Ohashi, Jpn J. Appl. Phys. **34**, 5349–5353 (1995)
9. S.J. Zhang, S. Rhee, C.A. Randall, T.R. Shrout, Jpn J. Appl. Phys. **41**, 722–726 (2002)
10. Y. Hosono, Y. Yamashita, H. Sakamoto, N. Ichinose, Jpn J. Appl. Phys. **41**, L1240–L1242 (2002)
11. R.E. Eitel, C.A. Randall, T.R. Shrout, P.W. Rehrig, W. Hackenberger, S.E. Park, Jpn J. Appl. Phys. **40**, 5999–6002 (2001)
12. C.J. Stringer, T.R. Shrout, C.A. Randall, I.M. Reaney, J. Appl. Phys. **99**, 024106 (2006)
13. C.A. Randall, R. Eitel, B. Jones, T.R. Shrout, D.I. Woodward, I.M. Reaney, J. Appl. Phys. **95**, 3633–3639 (2004)
14. V.V. Shvartsman, W. Kleemann, J. Dec, Z.K. Xu, S.G. Lu, J. Appl. Phys. **99**, 124111 (2006)
15. M.S. Yoon, H.M. Jang, J. Appl. Phys. **77**, 3991–4001 (1995)
16. G.C. Deng, A.L. Ding, G.R. Li, X.S. Zheng, W.X. Cheng, P.S. Qiu, Q.R. Yin, J. Appl. Phys. **98**, 094103 (2005)
17. X.H. Dai, Z. Xu, D. Viehland, J. Appl. Phys. **79**, 1021–1026 (1996)
18. J. Fu, R.Z. Zuo, Acta Mater. **61**, 3687–3694 (2013)
19. K. Uchino, S. Nomura, Ferroelectr. Lett. **44**, 55–61 (1982)
20. E.V. Colla, N.K. Yushin, D. Viehland, J. Appl. Phys. **83**, 3298–3304 (1998)
21. W.W. Cao, L.E. Cross, Phys. Rev. B **47**, 4825–4830 (1993)
22. A.A. Heitmann, G.A. Rossetti Jr., J. Am. Ceram. Soc. **97**, 1661–1685 (2014)
23. M. Iwata, H. Orihara, Y. Ishibashi, Jpn. J. Appl. Phys. 40, 708–712 92001)
24. T. Leist, T. Granzow, W. Jo, J. Rodel, J. Appl. Phys. **108**, 014103 (2010)
25. H.J. Lee, S.J. Zhang, J. Luo, F. Li, T.R. Shrout, Adv. Funct. Mater. **20**, 3154–3162 (2010)